

Analysis of Morphological and Morphometric Results of the Prostate Gland in 3-Month-Old White Outbred Rats with Experimentally Induced Pulmonary Fibrosis

Fayzullaev Komiljon Nabijonovich

Independent Researcher at Bukhara State Medical Institute, Uzbekistan

Abstract Introduction: This scientific study was conducted on white outbred rats of different ages with experimentally induced pulmonary fibrosis. In the study, bleomycin was administered endotracheally to 3-month-old white outbred rats, causing inflammation in the lungs and subsequently leading to pulmonary fibrosis. **Methods:** The dissertation research was conducted at the scientific research laboratory of Bukhara State Medical Institute from 2021 to 2024. For experimental studies, 86 white outbred male rats aged 3, 6, and 9 months were selected. The laboratory animals were kept in the vivarium of Bukhara State Medical Institute. In the scientific study, pulmonary inflammation and fibrosis were induced using the drug Bleomycin. **Conclusion:** Despite some anatomical and histological differences between human and white outbred rat prostate glands under normal conditions, numerous similarities were identified. The prostate gland of the control group of white outbred rats, anatomically distinct from the human prostate gland, consists of 4 separate lobes: anterior, lateral, ventral, and dorsal, based on the location of the excretory ducts in the urethra.

Keywords Experimental pulmonary fibrosis, Pneumosclerosis, Experimental animals, Rat prostate gland, Morphological and morphometric examination

1. Introduction

Currently, idiopathic pulmonary fibrosis is understood as a chronic progressive fibrotic interstitial aseptic pneumonia of unknown etiology. Idiopathic pulmonary fibrosis (IPF) plays an important role in the spectrum of interstitial lung diseases. IPF is a fatal disease characterized by a progressive decline in quality of life, increasing limitation of physical functions, and premature death from respiratory failure. [1].

The main virulence factor in the pathogenesis of COVID-19 is the interaction between the receptor-binding domain of the S protein, located on the outer membrane of the virus, and the angiotensin-converting enzyme 2 (ACE2) receptors. The development of COVID-19 is characterized by diffuse alveolar damage, which is determined by the formation of hyaline membranes, as well as the organization of alveolar exudate and interstitial fibrosis. [2]. The rate of inflammation and fibrosis development in the lungs is influenced not only by the volume and frequency of aspirations but also by the composition of aspirated materials. [3]. Thus, during the COVID-19 pandemic and due to various reasons, the development of idiopathic pulmonary fibrosis has been observed. [4]. Statistical data show that the reduction of pulmonary fibrosis and changes in the activity of other organs in the body

as a result of pulmonary fibrosis are observed to varying degrees. Taking this into account, the prevention of pathologies arising from morphological changes occurring in the prostate gland tissue is one of the urgent problems of modern urology. [5].

2. Methodology

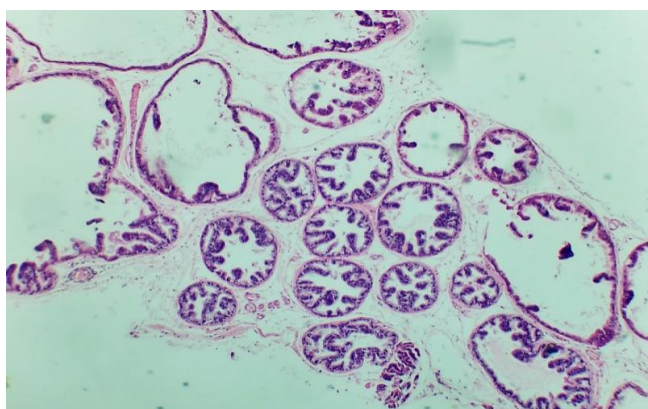
The dissertation research was conducted at the scientific research laboratory of Bukhara State Medical Institute from 2021 to 2024. For experimental studies, 86 white outbred male rats aged 3, 6, and 9 months were selected. The laboratory animals were kept in the vivarium of Bukhara State Medical Institute. In the scientific study, pulmonary inflammation and fibrosis were induced using the drug Bleomycin. The following group of rats received Bleomycin endotracheally 4 times (1.5 IU/kg body weight) over a period of 1 month. The main objects of the study were histological preparations made from the prostate gland of white outbred male rats. Hematoxylin-eosin staining was used for general morphological examination. Among histochemical research methods, the VAN-Gieson method was used to identify collagen fibers specific to connective tissue in the tissue composition. In morphometric studies, data were obtained from morphometric indicators such as prostate mass (mg), epithelial surface area (μm^2), stromal surface area (μm^2),

alveolar-tubular lumen surface area (μm^2), epithelial height (μm), epithelial width (μm), and number of binucleated epithelial cells (units).

3. Results

The prostate gland anatomically differs among various laboratory animals. The prostate gland is usually located under the urinary bladder and in front of the rectum. There are many similarities in the histological structure of the prostate gland in laboratory animals and humans, but anatomically, in white outbred rats, the prostate gland consists of several lobes. The anatomical structure of the prostate gland in white outbred rats consists of four lobes, which have morphologically different aspects. These are the ventral lobe, lateral lobe, dorsal lobe, and anterior lobe. The naming of these lobes is based on their location relative to the bladder opening into the urethra. Despite the anatomical differences between human and white outbred rat prostate glands, the similarities in their histological, functional, and molecular mechanisms allow for experimental studies of various prostate disease models that occur in humans using these laboratory animals.

The prostate gland of a white outbred rat is a tubular alveolar exocrine gland. It consists of four separate lobes: the dorsal prostate gland, the lateral prostate gland, the ventral prostate gland, and the anterior or coagulating gland, named after the location where their ducts open into the urethra. The above-mentioned parts have their own distinct histological features.

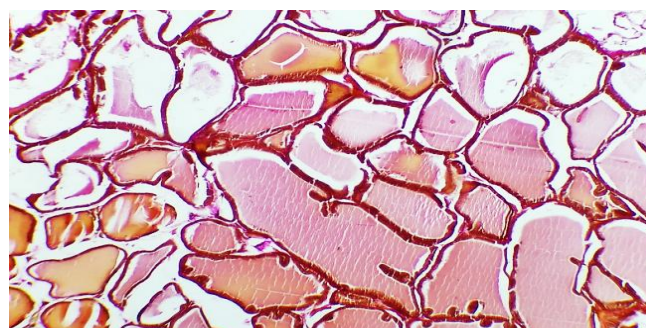


Figures 1. Prostate gland of a 3-month-old white outbred

Histologically, the lobules of the prostate gland are surrounded by a thin mesothelial connective tissue capsule. Each lobule consists of separate alveoli and acini, as well as numerous branching excretory ducts that empty into the urethra. Each acinus in the prostate contains thin, sparse connective tissue cells, smooth muscle cells, blood vessels, nerve fibers, nerve ganglia, macrophages, and mast cells. Additionally, secretory cells and basal cells are located in the acini and their excretory ducts. Basal cells do not produce secretions, and besides these cells, neuroendocrine cells are also present. The shape of secretory cells varies from

cuboidal to columnar, depending on their secretory activity. The secretory activity and elasticity of the gland cause changes in the height of the cells in the acini. The acini are surrounded by smooth muscle fibers, and the complex contraction of these muscles facilitates the release of prostate gland secretions from the acini into the urethra through the excretory ducts.

Microscopic view of a preparation obtained from the anterior lobe of the prostate gland of a 3-month-old white outbred rat in the control group. Stained with hematoxylin and eosin, magnified 200 times. Alveolar-tubular glands forming the parenchyma of the prostate gland (1). Blood vessels (2). Fibromuscular stroma of the organ (3).



Figures 2. Fine collagen fibers in the basal layer and stroma of the prostate gland

Microscopic view of the prostate gland of a 6-month-old white outbred rat in the control group. Stained using the Van Gieson method, magnified 100 times. Fine collagen fibers in the basal layer and stroma of the prostate gland (1). When studying the morphometric indicators of 3-month-old white outbred rats obtained in the experimental control group, the following results were established (see Table 1). When studying the morphometric parameters of 3-month-old white outbred rats in the control group, the following results were revealed: the average mass of the prostate gland was 124.32 ± 2.75 mg, the area of epithelial cells was $1584.08 \pm 261.17 \mu\text{m}^2$, the area of the stroma was $1685.28 \pm 376.12 \mu\text{m}^2$, the area of the alveolar-tubular space was $11307.45 \pm 2069.24 \mu\text{m}^2$. The height of epithelial cells was $17.84 \pm 0.53 \mu\text{m}$, the width of epithelial cells was $14.03 \pm 0.29 \mu\text{m}$, and the number of binuclear epithelial cells averaged 0.76 ± 0.12 (see Fig. 3).

Table 1. Morphometric indicators of the prostate gland in 3-month-old white outbred rats of the control group

Morphometric indicators	Control group
Prostate mass (mg)	124.32 ± 2.75
Epithelial surface area (μm^2)	1584.08 ± 261.17
Stromal surface area (μm^2)	1685.28 ± 376.12
Alveolar-tubular lumen surface area (μm^2)	11307.45 ± 2069.24
Epithelial height (μm)	17.84 ± 0.53
Epithelial width (μm)	14.03 ± 0.29
Number of binucleated epithelial cells (units)	0.76 ± 0.12

Note: * - compared to "3 months" (** - $P < 0.05$; ** - $P < 0.01$; * - $P < 0.001$);



Figure 3. Shows the morphometric measurements of the prostate gland in 3-month-old white outbred rats from the control group

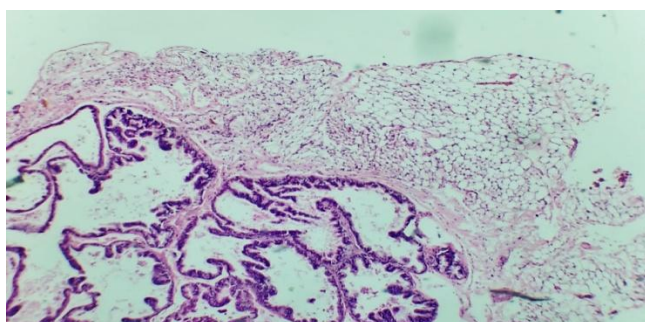


Figure 4. Shows a microscopic view of a preparation taken from the anterior lobe of the prostate gland of a 3-month-old white outbred rat in the experimental group with induced pulmonary fibrosis. Stained with hematoxylin and eosin, magnified 100 times. Increased amount of adipose tissue surrounding the prostate gland (1). Congestion and flattening of epithelial folds in the alveolar-tubular glands that make up the parenchyma of the prostate gland (2)

The morphological and morphometric results of the prostate gland in 3-month-old white outbred rats from the experimental group with induced pulmonary fibrosis were as follows. In the study, lung tissue samples were initially taken and analyzed from white outbred rats in the group with induced pulmonary fibrosis. After histological confirmation of signs of pulmonary fibrosis of varying degrees in almost all of the selected rats, prostate gland samples from these same rats were examined, and the following results were obtained. Macroscopically, it was found that in 3-month-old rats, the amount of fatty tissue surrounding the prostate gland from the posterior side had increased. The capsule was slightly thickened, and its transparency was somewhat reduced. The blood vessels located in the subcapsular region appeared slightly dilated. The prostate gland consists of dorsal, ventral, lateral, and anterior lobes. In some samples, a slight enlargement of the gland, increased tension of the capsule, and a slight hardening of consistency were observed. This condition was noted in almost all dissected sections, but was more prominent and studied in the dorsal lobe of the prostate gland. Microscopic analysis of the results showed uneven thickening of the capsule surrounding the prostate gland. In the subcapsular blood vessels, especially in the veins,

signs of increased blood volume, i.e., congestion, were present. Various degrees of venous congestion were observed. The blood vessel walls were slightly thickened, and within the blood vessels, blood formed elements, particularly erythrocytes, were positioned closer together, adhering to each other. This is characteristic of slowed blood flow, known as stasis.

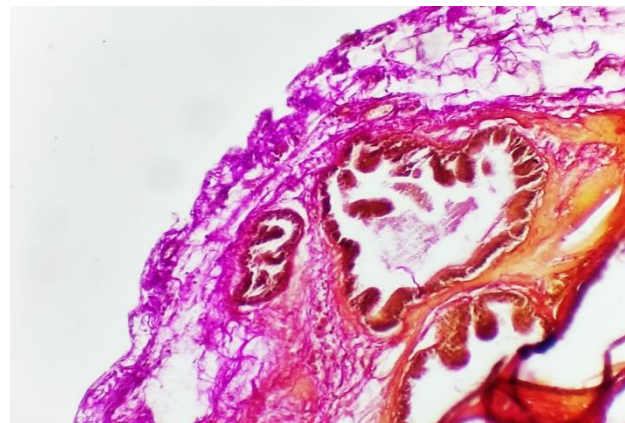


Figure 5. Shows a microscopic view of a preparation obtained from the anterior lobe of the prostate gland of a 3-month-old white outbred rat in the experimental group with induced pulmonary fibrosis. Stained with hematoxylin and eosin, magnified 100 times. An increase in the amount of densely packed collagen fibers under the capsule surrounding the prostate gland and around the acini (1)

The following morphometric indicators were observed in 3-month-old white outbred rats from the experimental pulmonary fibrosis group (see Table 2).

Table 2. Morphometric parameters of the prostate gland in 3-month-old white outbred rats of the pulmonary fibrosis group

Morphometric indicators	3-month
Prostate mass (mg)	137.25±2.34
Epithelial surface area (μm ²)	1523.11±261.17
Stromal surface area (μm ²)	1712.16±376.12
Alveolar-tubular lumen surface area (μm ²)	11334.27±1921.17
Epithelial height (μm)	17.62±0.31
Epithelial width (μm)	13.95±0.31
Number of binucleated epithelial cells (units)	0.82±0.14

Note: * - compared to "3-month" (*** - P<0.05; ** - P<0.01; * - P<0.001);

In the experiment, histomorphometric and cytomorphometric indicators of the prostate gland in 3-month-old white outbred rats with induced pulmonary fibrosis revealed the following results: the average mass of the prostate gland was 137.25±2.34 mg, the area of epithelial cells was 1523.11±261.17 μm², the area of the stroma was 1712.16±376.12 μm², and the area of the alveolar-tubular space was 11334.27±1921.17 μm². The height of epithelial cells was 17.62±0.31 μm, the width of epithelial cells was 13.95±0.31 μm, and the average number of binuclear epithelial cells was 0.82±0.14.

4. Conclusions

Despite some anatomical and histological differences

between human and white outbred rat prostate glands under normal conditions, numerous similarities were identified. The prostate gland of the control group of white outbred rats, anatomically distinct from the human prostate gland, consists of 4 separate lobes: anterior, lateral, ventral, and dorsal, based on the location of the excretory ducts in the urethra. Although there are some histological differences in the structure of these lobes, the similarity in their histological structure, molecular mechanisms, and functional properties allows for the study of prostate diseases in experiments using these laboratory animals.

Macroscopically, an increase in the amount of fatty tissue surrounding the prostate gland, thickening and opacity of the capsule surrounding the gland, and signs of congestion in the blood vessels located under the capsule were observed. Microscopically, the prostate gland capsule was unevenly thickened, with congestion in the blood vessels, especially in the veins. The vessel walls were thickened, and signs of intravascular stasis were noted. An increase in interstitial edema, leukocyte cells, and collagen fibers was revealed in the gland stroma. In the glandular acini, flattening of the epithelial folds was observed, along with a decrease in the height of epithelial cells, which took on a cuboidal shape. There was a decrease in vesicles on their apical surfaces, as well as signs of congestion of glandular secretion in the acini and small concretions in some areas.

In the experiment, it was established that in the group with induced pulmonary fibrosis, compared to the control group, the mass of the gland increased by 9.5% at 3 months, the surface area of the stroma increased by 6.5% at 3 months, and the surface area of the alveolar cavity increased after 3 months. It was found that the height of epithelial cells decreased by 2% at 3 months, and the width decreased by 0.5% at 3 months, while the surface area of epithelial cells in the tissue decreased by 4% at 3 months. The number of binucleated epithelial cells increased by 7% at 3 months. These morphometric indicators show that pulmonary fibrosis has a significant effect on the histological structures of the prostate gland.

Funding

This research did not receive any specific grant from funding agencies in the public, commercial, or not-for-profit sectors.

Declaration of Competing Interests

All the authors declare no conflict of interest.

CRedit Authorship Contribution

The authors would like to thank the Bukhara State Medical Institute for supporting this study and providing the data through the Bukhara State Medical Institute Central Library.

Ethics Approval and Consent to Participate

Not applicable.

REFERENCES

- [1] Avdeev S.N., Gainitdinova V.V., Merzhoeva Z.M. and others. Exacerbation of idiopathic pulmonary fibrosis // *Therapeutic Archive*. 2020; 92(3): 73– 77. [Avdeev S.N., Gaynitdinova V.V., Merjoyeva Z.M. et al. Execution of idiopathic pulmonary fibrosis // *Therapeutic Archive*. 2020; 92 (3): 73-77.]
- [2] Avdeev S.N. Idiopathic pulmonary fibrosis // *Pulmonology*. 2016; 25: 5: 600-612. [Avdeev S.N. Idiopathic pulmonary fibrosis // *Pulmonology*. 2016; 25 (5): 600-612.]
- [3] Avdeev S.N. Idiopathic pulmonary fibrosis // *Consilium Medicum*. 2017; 19(3): 17-23. Alyaev Yu. G. and others. Kidney tumor and urolithiasis: is there a relationship? // *Urology*. - 2016. – No. 3. – pp. 104-107. [Avdeev S.N. Idiopathic pulmonary fibrosis // *Consilium Medicum*. 2017; 19 (3): 17-23. Alyaev Yu. G. et al. Kidney tumor and urolithiasis: is there a correlation? // *Urology*. 2016; (3): 104-107.]
- [4] Strizhakov A.P. Idiopathic pulmonary fibrosis // *Handbook of a general practitioner*. 2017; 9: 46-54. [Strizhakov A.P. Idiopathic pulmonary fibrosis // *Титова О.Н., Суховская О.А., Куликов В.Д. Курение табака и интерстициальные заболевания легких (обзор литературы) // Практическая пульмонология*. 2019; 1: 32-37. [Titova O.N., Sukhovskaya O.A., Kulikov V.D. Tobacco smoking and interstitial lung diseases (literature review) // *Practical Pulmonology*. 2019; 1: 32-37.]
- [5] Li W., Li X., Zhang B. et al. Current progress and trends in the development of progesterone receptor modulators. *Curr Med Chem* 2016; 23 (23): 2507-54. DOI: 10.2174/0929867323666160428105310.